中国光学 Chinese Optics 核心期刊

基于碳纳米薄膜/砷化镓范德华异质结的高性能自驱动光电探测器研究

霍婷婷 张冬冬 施祥蕾 潘宇 孙利杰 苏言杰

High-performance self-powered photodetectors based on the carbon nanomaterial/GaAs vdW heterojunctions

HUO Ting-ting, ZHANG Dong-dong, SHI Xiang-lei, PAN Yu, SUN Li-jie, SU Yan-jie

引用本文:
霍婷婷, 张冬冬, 施祥蕾, 潘宇, 孙利杰, 苏言杰. 基于碳纳米薄膜/砷化镓范德华异质结的高性能自驱动光电探测器研究[J]. 中国光学, 2022, 15(2): 373–386. doi: 10.37188/CO.2021–0149
HUO Ting-ting, ZHANG Dong-dong, SHI Xiang-lei, PAN Yu, SUN Li-jie, SU Yan-jie. High-performance self-powered photodetectors based on the carbon nanomaterial/GaAs vdW heterojunctions[J]. *Chinese Optics*, 2022, 15(2): 373-386. doi: 10.37188/CO.2021-0149

在线阅读 View online: https://doi.org/10.37188/CO.2021–0149

文章编号　2095-1531(2022)02-0373-14

High-performance self-powered photodetectors based on the carbon nanomaterial/GaAs vdW heterojunctions

HUO Ting-ting[1], ZHANG Dong-dong[2], SHI Xiang-lei[3], PAN Yu[3], SUN Li-jie[3*], SU Yan-jie[1*]

(1. *Key Laboratory of Thin Film and Microfabrication (Ministry of Education)*, *Department of Micro/Nano Electronics*, *School of Electronics Information and Electrical Engineering*, *Shanghai Jiao Tong University*, *Shanghai* 200240, *China*;

2. *Shanghai Academy of Spaceflight Technology*, *Shanghai* 201109, *China*;

3. *State Key Laboratory of Space Power Technology*, *Shanghai Institute of Space Power Sources*, *Shanghai* 200245, *China*)

* *Corresponding author*, *E-mail*: *sunlijielu*@163.*com*; *yanjiesu@sjtu.edu.cn*

Abstract: With the advantages such as simple structure, simple process and easy interface control, the photoelectric devices based on carbon nanomaterial/bulk semiconductor van der Waals (vdW) heterojunctions can fully realize the ultrahigh carrier mobility of carbon nanomaterials and the excellent photoelectric properties of bulk semiconductors. Especially, the novel mixed-dimensional vdW heterojunctions can be prepared by controlling the diameter/chirality and Fermi level of single-walled carbon nanotubes (SWCNTs) to form atomic-level interfaces and match bandgaps with bulk semiconductors. Here, we reported a self-powered broadband photodetector based on the pn vdW heterojunctions by combining (6, 5)-enriched semiconducting SWCNT film with n-type GaAs, and used graphene to reduce the probability of carrier recombination in SWCNT film and to promote the carrier transport. The experimental results suggest that the self-powered device exhibits high-sensitivity photoelectric response toward the incident photons in the 405~1 064 nm range, and that the max photoelectric responsivity of 1.214 A/W and the specific detectivity of 2×10^{12} Jones could be achieved at zero bias.

Key words: van der Waals heterojunctions; single-walled carbon nanotubes; GaAs; self-powered photodetectors

收稿日期:2021-07-23; **修订日期**:2021-08-26

基金项目:国家自然科学基金 (No. 61974089); 上海市自然科学基金 (No. 19ZR1426900)

Supported by National Natural Science Foundation of China (No. 61974089); Shanghai Natural Science Foundation (No. 19ZR1426900).

基于碳纳米薄膜/砷化镓范德华异质结的高性能自驱动光电探测器研究

霍婷婷[1], 张冬冬[2], 施祥蕾[3], 潘　宇[3], 孙利杰[3*], 苏言杰[1*]
（1. 上海交通大学 电子信息与电气工程学院 微纳电子学系
薄膜与微细技术教育部重点实验室，上海 200240；
2. 上海航天技术研究院，上海 201109；
3. 上海空间电源研究所空间电源技术国家重点实验室，上海 200245）

摘要: 基于碳纳米材料/体半导体范德华(vdW)异质结的光电器件可以同时实现碳纳米材料的超高载流子迁移率以及体半导体的优异光电性能，且具有结构简单、工艺简便、易于调控界面等优点。尤其是通过调控单壁碳纳米管(SWCNT)的直径/手性、费米能级等可以与体半导体形成能带匹配、具有原子级界面的新型混合维度 vdW 异质结。本文报道了一种基于(6, 5)手性为主的 SWCNT 薄膜与 n 型 GaAs 所形成的 pn 结的宽光谱自驱动光电探测器，并利用石墨烯降低 SWCNT 薄膜内载流子的复合几率和促进载流子传输。实验结果表明，器件对 405~1 064 nm 波段光子表现出高灵敏的光电响应，零偏压条件下最大光电响应度和比探测率分别可达 1.214 A/W 和 2×10^{12} Jones。

关　键　词: 范德华异质结；单壁碳纳米管；砷化镓；自驱动光电探测器
中图分类号: TN362　　**文献标志码:** A　　**doi:** 10.37188/CO.2021-0149

1 Introduction

As a typical quasi-one-dimensional nanomaterial, Single-Walled Carbon NanoTubes (SWCNTs) can exhibit semiconduct or metallic according to their diameter and chirality. Moreover, the semiconducting SWCNT has a direct bandgap that is inversely proportional to its diameter[1-2]. SWCNT is widely applied to construct high-performance photoelectric devices owing to its ultra-high carrier mobility (10^5 cm^2/Vs), high absorption coefficient (10^4−10^5/cm) and long exciton diffusion length[3-5]. However, strong Coulomb interaction results in the existence of photogenerated electron/hole pairs in the form of excitons after the SWCNT absorbs photons. The exciton binding energy of several hundred meV is directly affected by the SWCNT diameter[6-8]. In order to promote effective exciton separation, the application of strong electric fields or the fabrication of heterojunctions is usually pursued to establish strong built-in electric fields. In particular, the strategy of building heterojunctions with other materials, such as bulk semiconductors, nanomaterials and polymers, is widely used to enhance exciton separation and carrier transport[9-16].

With the advantages such as simple structure, simple process and easy interface control, the SWCNT/n-type bulk semiconductor vdW heterojunction, a type of SWCNT-based heterojunction, can fully utilize the ultrahigh carrier mobility of SWCNT and the excellent photoelectric properties of bulk semiconductors[12-18]. More importantly, this novel device has broken through the limitation of lattice matching in the growth process of traditional p-n junctions. It can also avoid the disorder interface structure caused by mutual atom diffusion during the formation of vdW heterojunctions, thus facilitating the separation and transport of photogenerated carriers at the interface[19-20]. Therefore, the photoelectric devices based on SWCNT/bulk semiconductor vdW heterojunctions are expected to exhibit higher photoelectric response[17-18]. In addition, the novel mixed-dimensional vdW heterojunctions with atomic-level interfaces, whose bandgaps are matched with those of bulk semiconductors, can be formed by controlling the diameter/chirality and Fermi level of SWCNTs to facilitate the develop-

ment of new wide-spectrum photoelectric devices with higher performance.

Different from indirect bandgap semiconductor silicon, gallium arsenide (GaAs) is a direct bandgap semiconductor with better photoelectric performance, more suitable bandgap and higher carrier mobility, and has been widely used in high-efficiency space solar cells. Therefore, the photoelectric devices based on SWCNT/GaAs vdW heterojunctions are expected to exhibit higher photoelectric response than those based on silicon vdW heterojunctions. Liang et al[21]. first proved the existence of strong rectification performance in a single SWCNT/n-GaAs heterojunction, and observed obvious photovoltaic effect under irradiation condition. This has laid a foundation for the development of high-performance self-powered SWCNT/GaAs photodetectors. Li et al[22]. reported the photovoltaic response of a single SWCNT/n-type GaAs heterojunction. They found that the carrier transport was dominated by thermoelectron emission at low forward bias, while the hole tunneling in the pass interband state mainly contributed to electric current at low reverse bias. Behnam et al[23]. studied the Metal-Semiconductor-Metal (MSM) photodetector based on SWCNT film/GaAs Schottky contact, and found that thermoelectron emission was the main transmission mechanism in the SWCNT film/GaAs heterojunction at a temperature above 260 K. The detector exhibited 0.161 A/W photoresponsivity and high switching ratio under 633 nm laser irradiation and 10 V bias.

However, the presence of the SWCNTs with different diameters or mixed conductive properties can easily lead to the non-radiative recombination of carriers in the films, and reduce the separation and transmission efficiency of photogenerated carriers. Therefore, we fabricated a self-powered photodetector based on the p-n vdW heterojunctions by combining (6, 5) enriched SWCNT film with n-type GaAs, and graphene is used to reduce the probability of carrier recombination in SWCNT film and to promote the carrier transport. We tested in detail the wide-spectrum response characteristics of the device in the visible-near infrared band at zero bias. Our results also verify the feasibility of fabricating high-efficiency solar cells based on the vdW heterostructures.

2 Experiment

2.1 SWCNT film preparation

SWCNT film has been prepared by vacuum extraction and filtration[24]. The specific steps are described as follows. Firstly, 0.5 mg (6, 5)-enriched SWCNT powder (purchased from Sigma-Aldrich) was dispersed into aqueous sodium dodecyl sulfate (SDS) solution (0.01 g/mL) using low-temperature ultrasonic treatment for 2 h. The mixed solution was centrifuged at 14 000 r/min for 20 min to remove the inadequately dispersed SWCNT powder. Then, 10 mL centrifuged supernatant was gradually added to the vacuum filtration device with cellulose film (0.22 μm) for filtration and membrane formation. After the mixed solution was filtered, excessive deionized water was added to clean the excess SDS in SWCNT film to reduce its influence on the conductivity of SWCNT film. Finally, the (6, 5)-enriched SWCNT film on cellulose film was dried in a 40°C vacuum oven for 2 h.

2.2 Fabrication of graphene/SWCNT/GaAs vdW heterojunction photodetectors

In this paper, a photoelectric device with vdW heterojunctions was fabricated on a single-side polished n-type GaAs substrate (10 mm×10 mm, 20 μm) with AuGeNi eutectic alloy (4 μm) electrode deposited on its back. Firstly, the GaAs substrate was cleaned with acetone, isopropyl alcohol and deionized water successively to remove surface oil stains. Then, an 80 nm Al_2O_3 insulation layer was deposited on the significant surface of GaAs substrate by atomic layer deposition technology, and a 3 mm×3 mm window was opened in its middle. Subsequently, the GaAs substrate was immersed in $(NH_4)_2S$ solution for 30 min to passivate the GaAs surface within the window, and excess $(NH_4)_2S$

solution was removed with deionized water. Later, the prepared SWCNT film (7 mm×7 mm) was transferred above the patterned window and directly contacted with GaAs to form the SWCNT/GaAs vdW heterojunctions, and the cellulose film was dissolved and removed by slowly dripping acetone. The graphene was then transferred to the upper surface of SWCNT film by wet process. Finally, the graphene /SWCNT/GaAs vdW heterojunction photodetector was obtained by applying silver paste on the graphene surface around the window to form ohmic contact.

2.3 Testing and characterization

The surface morphologies of the graphene/SWCNT film/GaAs vdW heterojunction were characterized by Scanning Electron Microscopy (SEM) (Zeiss Ultra Plus, Germany). The Raman peak shift of the heterojunction was performed Via Renishaw Raman spectroscopy with an excitation wavelength of 514 nm. The photoelectric performance of the device was evaluated using Agilent 4156C semiconductor parameter analyzer at room temperature, and the current-voltage (*I*-*V*) curve and current-time (*I*-*T*) curve were measured by irradiation with 405−1 064 nm laser and AM1.5G standard solar simulator. The frequency response curve of the device was measured by a chopper (4−400 Hz) and a digital oscilloscope (Tektronix, TDS 3052C).

3 Result and discussion

The structure of the fabricated graphene/SWCNT film/GaAs vdW heterojunction photodetector is shown in Figure 1(a). It can be clearly seen that this is a p-n heterojunction structure directly formed by (6, 5)-enriched SWCNT film and n-type GaAs, significantly different from the previous SWCNT network/graphene/GaAs heterojunction photodetector, which is a Schottky heterojunction[25]. In this paper, the use of (6, 5)-enriched SWCNT film can improve the absorption of photons in bands smaller than GaAs bandgap. On the other hand, the Fermi level of SWCNT film can be later regulated by doping to better facilitate the fabrication of high-performance wide-spectrum photodetectors. Here, graphene mainly plays a role in promoting the transport of photogenerated carriers in the SWCNT film. Figure 1(b) shows a typical SEM image of graphene/SWCNT film/GaAs vdW heterojunction surface in the window area. It can be clearly seen that SWCNT and graphene forms a uniform meshed film on the GaAs surface, and no obvious residue of surfactant SDS is observed, indicating that the SDS removal is relatively thorough in the process of SWCNT film filtration. This will help improve the photoelectric performance of vdW heterojunction devices.

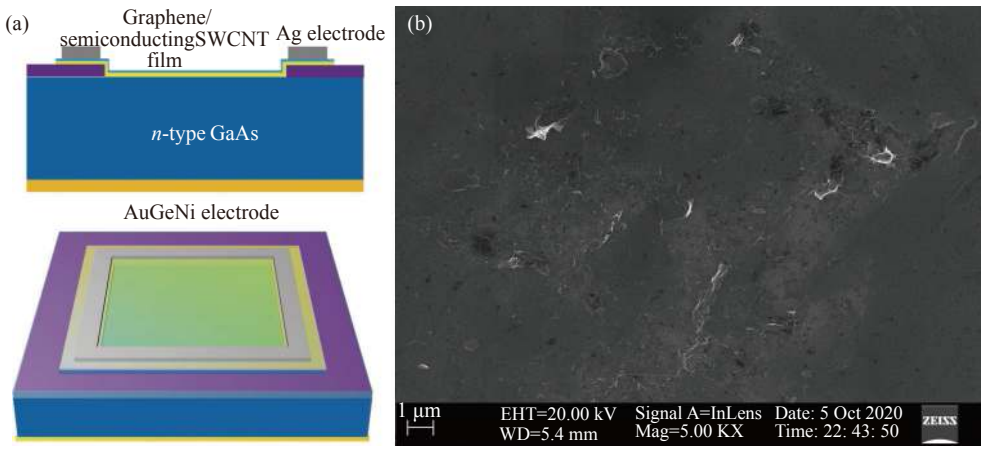

Fig. 1 (a) Schematic diagram of graphene/SWCNT film/GaAs vdW heterojunction photodetector structure; (b) SEM image of graphene/SWCNT film

图 1 (a)石墨烯/SWCNT 膜/GaAs vdW 异质结光电探测器结构示意图;(b)石墨烯/SWCNT 薄膜的 SEM 图片

We first tested the *J-V* curve of the graphene/SWCNT film/GaAs vdW heterojunction photodetector in dark state and AM1.5G light condition, as shown in Figure 2. It can be clearly seen from the *J-V* curve for dark state that the device has an obvious rectification effect, indicating that the (6, 5)-enriched SWCNT film is combined with GaAs into a good p-n junction in the device. It should be noted that the current density of device in the first quadrant is low. Under the AM1.5G standard solar radiation, the *J-V* curve obviously moves downward, and the short-circuit current density (J_{sc}) of device rises up to 19 mA/cm^2, an indicator of excellent photovoltaic performance. This indicates that the device has the potential to build efficient solar cells. The rectification performance of the device is analyzed based on the classical thermoelectron emission principle:

$$J = J_{st}[\exp\left(\frac{qV}{nk_0T}\right) - 1] \quad , \qquad (1)$$

$$J_{st} = A^*T^2\exp\left(-\frac{q\phi_{ns}}{nk_0T}\right) \quad , \qquad (2)$$

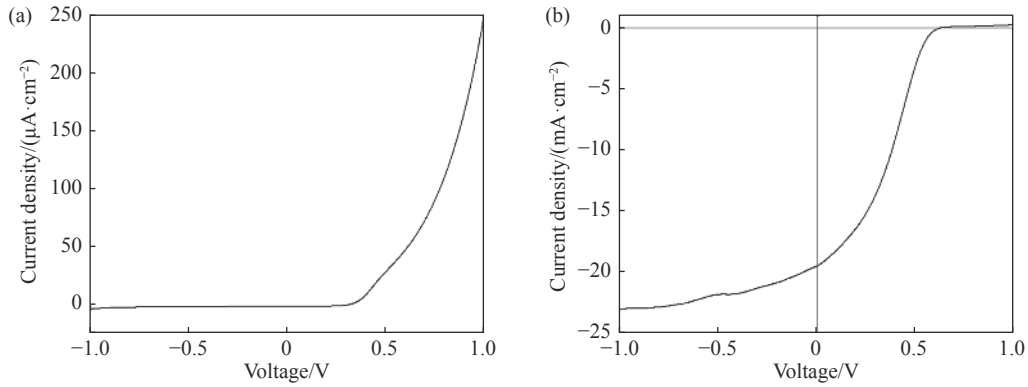

Fig. 2　Typical *J-V* curves of graphene/SWCNT film/GaAs vdW heterojunction photodetector in (a) dark state and (b) AM 1.5G condition

图 2　石墨烯/SWCNT 膜/GaAs vdW 异质结光电探测器在 (a) 暗态和 (b)AM 1.5G 条件下的 *J-V* 曲线

where J_{st} is the reverse saturation current density, T is the absolute temperature, k_0 is Boltzmann constant, A^* is the effective Richardson constant, and Φ_{ns} is the barrier height. From the *J-V* curve for dark state, it can be concluded that the saturation current density (J_{st}) is 9.93×10^{-7} A/cm^2, and that the thermoelectron emission plays a dominant role in carrier diffusion and generation recombination. However, the increase of current density drops sharply in the first quadrant, which may be related to the existence of the reverse junction. As a result, the *J-V* curve of the device is different from the existing result, but the open-circuit voltage is not significantly affected and is still 0.63 V. Therefore, the graphene/SWCNT film/GaAs vdW heterojunction is mainly viewed as a self-powered photoelectric device and is evaluated in terms of detection performance.

In order to evaluate the detection performance of the graphene/SWCNT film/GaAs vdW heterojunction devices as self-powered photodetectors, we measured the photoelectric response at different laser wavelengths at room temperature, as shown in Figure 3 (Color online). Figure 3(a)~(b) shows the typical *J-V* curves of the graphene/SWCNT film/GaAs vdW heterojunction photodetectors under laser irradiation at different wavelengths. It can be clearly seen that all *J-V* curves move downward at different laser wavelengths, indicating that the vdW heterojunction devices exhibit obvious photovoltaic effect. In particular, the maximum short-circuit current density (J_{sc}) of the device can reach 22.48 mA/cm^2 under the irradiation of 405 nm laser with 30 mW/cm^2 optical power density. It is worth

noting that the device can still produce a relatively obvious photovoltaic effect under 1 064 nm laser irradiation. The downward shift of *J-V* curve to break through the 860 nm absorption limit of GaAs is mainly caused by the existence of (6, 5)-enriched SWCNT film in the heterojunction. Thus, the photo-induced carriers generated by (6, 5)-enriched SWCNT film after absorbing photons can be separated into electron-hole pairs at the heterojunction interface and exported to the external circuit to form a photocurrent dominating the photoelectric response process of the device. The introduction of graphene can help enhance the transport of holes in the SWCNT film and improve the ability of charge collection. Therefore, the subsequent optimization of graphene, the thickness and Fermi level of SWCNT film, bandgap and the SWCNT-GaAs interface contact will be expected to further improve the photoelectric response characteristics in long-wave band. Figure 3(c)~(d) shows the stability curves of the graphene/SWCNT film /GaAs vdW heterojunction photodetector irradiated at different laser wavelengths. It can be clearly seen that the photocurrent density increases or decreases rapidly with the laser on or off, and the device exhibits fast photoelectric response and excellent photoelectric response stability under 405−1 064 nm laser illumination. Moreover, the device shows a high switching ratio, which is greater than 1.1×10^3 under 406~860 nm laser illumination and is 2.5 even when irradiated by 1 064 nm laser.

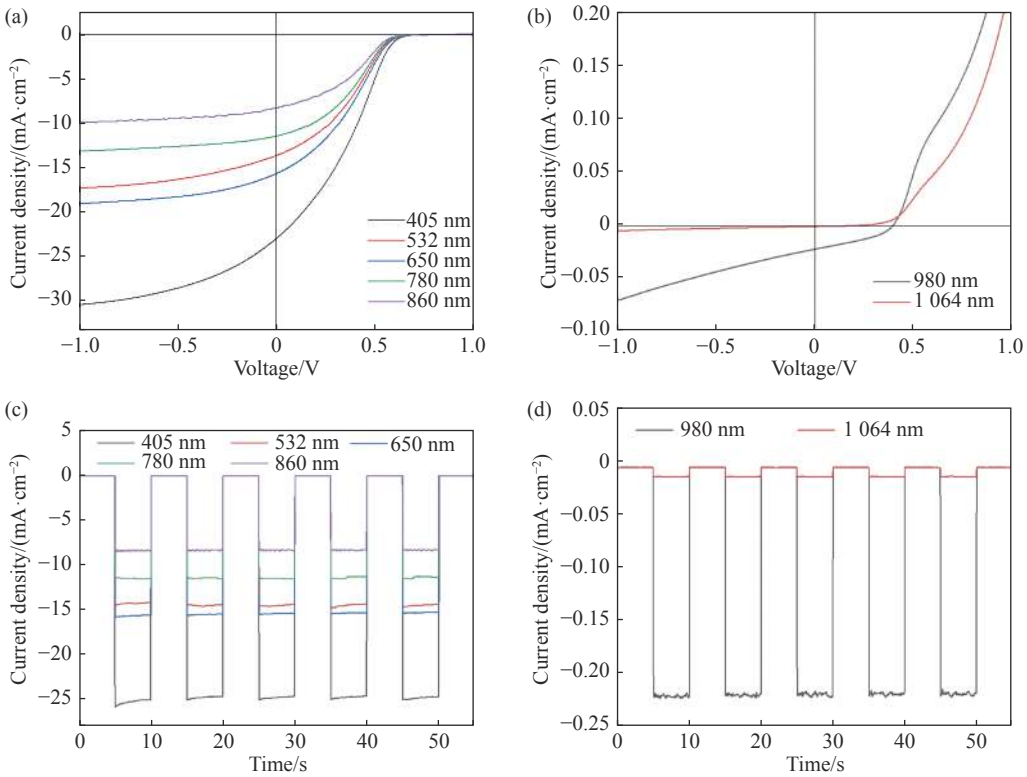

Fig. 3 (a) (b) *J-V* curves of the graphene/SWCNT film/GaAs vdW heterojunction photodetector irradiated at different laser wavelengthes. (c) (d) Photoelectric response repeatability curves when irradiated by laser with different laser wavelengthes at zero bias

图 3 (a) 和 (b) 不同激光波长辐照下石墨烯/SWCNT 膜/GaAs vdW 异质结光电探测器的 *J-V* 曲线; (c) 和 (d) 零偏压时不同激光波长辐照下的光电响应重复性曲线

In addition, we tested the transient light response of the device at 200 Hz frequency and

405 nm laser wavelength, as shown in Figure 4. It can be seen that the photodetector shows a fast response speed when switching the on/off state. The photoelectric response curve is still complete at the frequency of 200 Hz. When the frequency is further increased, the photoelectric response of the photodetector begins to decline before reaching a maximum. Thus, the maximum response frequency of the self-powered photoelectric device based on graphene/SWCNT film/GaAs vdW heterojunction is 200 Hz. In addition, the photoelectric response time of the device can be extracted from the photoelectric response curve. In general, the response (t_r)/recovery (t_f) time of the device is defined as the time required for the photoelectric current to rise/fall to 90%/10% of the maximum photocurrent, respectively. From Figure 4, the response (t_r)/recovery (t_f) time can be determined as 60 μs and 910 μs, respectively. The response time of tens of microseconds indicates the ultra-fast carrier separation efficiency at the SWCNT/GaAs interface and the ultra-high charge transport efficiency of the whole graphene/SWCNT film/GaAs vdW heterojunction photodetector.

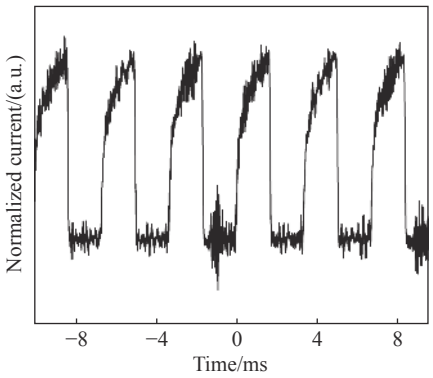

Fig. 4　Transient light response curve of the device under 405 nm laser irradiation

图 4　405 nm 激光辐照条件下器件的瞬态光响应曲线

We further evaluated the photoelectric responsivity (R) and specific detectivity (D^*) of the graphene/SWCNT film/GaAs vdW heterojunction photodetector. The R and D^* values at different laser wavelengthes can be obtained according to the following formula:

$$R_\lambda = \frac{I_p - I_d}{P_{in}} \quad , \tag{3}$$

$$D^* = \sqrt{\frac{A}{2qI_d}} R_\lambda \quad , \tag{4}$$

where I_p is the photocurrent, I_d is the dark current, P_{in} is the incident light power, and A is the effective area (9 mm^2). By changing the laser wavelength and incident power density, the change values of R and D^* values of the graphene/SWCNT film/GaAs vdW heterojunction photodetector are obtained, as shown in Figure 5. It can be seen from the photoelectric response curves in Figure 5(a)−(b) that the photoelectric responsivity of the device increases as a whole with decreasing the incident power density. This change trend basically accords with the general law of photo detector, this is because the incident light can be absorbed by the device and be fully converted into current with the decrease of the incident power. From Figure 5(a), the maximum R value of the self-powered photodetector under 405 nm laser irradiation can reach 1 214 mW/cm^2, which is higher than the values reported in previous studies[24]. Although the photoelectric response of the device at 980−1 064 nm is 3 orders of magnitude lower than that at 405−860 nm, this result still demonstrates the feasibility that the graphene/SWCNT film/GaAs vdW heterojunctions fabricated in this paper can further broaden the spectral response range. Subsequently, high photoelectric responsivity can be expected at 405−1 064 nm by optimizing the relative thickness of SWCNT and GaAs until their light absorption is of the same order of magnitude. Figure 5(c)~(d) shows the specific detectivity curves of the device under different laser wavelengths and optical power densities. Similar to the photoelectric responsivity, the specific detectivity also increases as a whole with decreasing incident power density, and the maximum specific detectivity of 2×10^{12} Jones can be obtained at 405 nm laser wavelength with the power density of 5 mW/cm^2.

In order to better understand the working mechanism of the graphene/SWCNT film/GaAs vdW

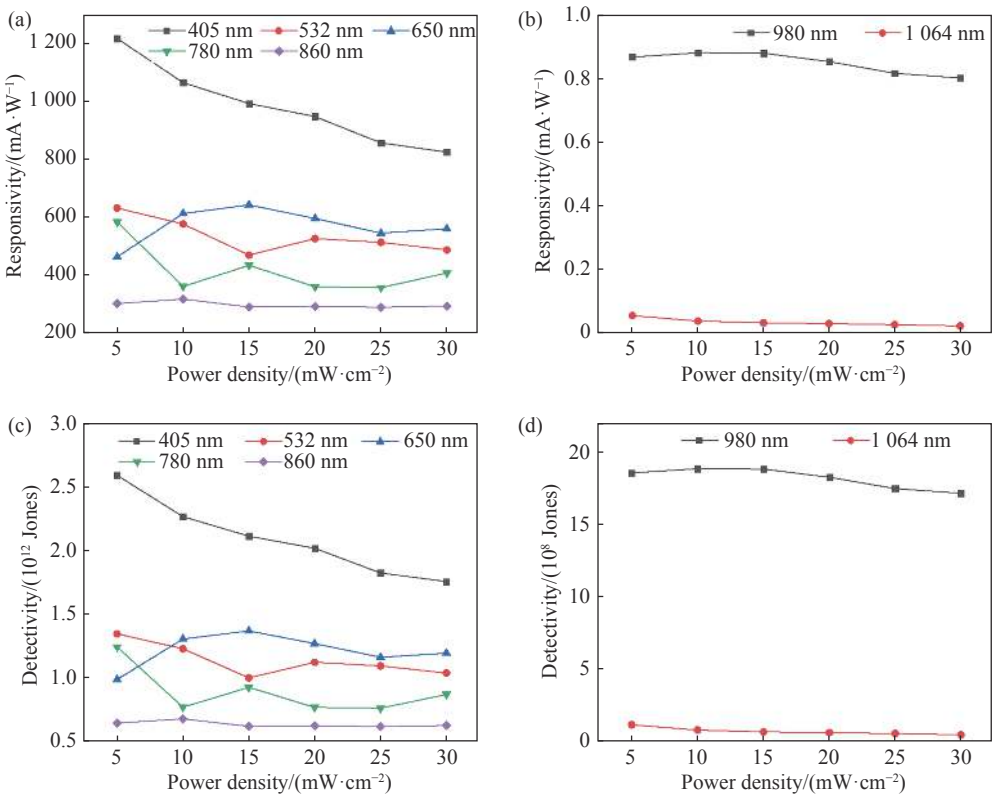

Fig. 5 The responsivity (a~b) and specific detectivity (c~d) of graphene/SWCNT film/GaAs vdW heterojunction photodetectors as a function of incident light power density under zero bias conditions

图 5 零偏压条件下石墨烯/SWCNT 膜/GaAs vdW 异质结光电探测器的 (a~b) 光电响应度和 (c~d) 比探测率随入射光功率密度改变而变化的曲线

heterojunction photodetector, we analyze the energy band structure and charge transfer process at the interface. Since the SWCNTs used in this paper is a (6, 5)-enriched semiconducting SWCNTs, the energy band structure of (6, 5) SWCNTs is used to analyze the energy band structure of SWCNT/GaAs heterojunction and its working mechanism is discussed. As we know, the Dirac point of graphene is 4.6 eV, and (6, 5) SWCNT exhibits a weak p-type with a conduction band of 3.9 eV and a valence band of 5.1 eV. The Fermi level of n-type GaAs is close to its 4.07 eV conduction band, and the energy band structure of the vdW heterojunction is shown in Figure 6. When (6, 5) SWCNT contacts with n-type GaAs, a II-type heterojunction can be formed due to the difference between their conduction bands and valence bands. According to the band theory, the static electron transfer from n-type GaAs to (6, 5) SWCNT happens after the contact, which can be confirmed by Raman spectrum[24]. A built-in electric field is formed between graphene/(6, 5) SWCNT and n-type GaAs, resulting in the bending of their energy bands. When the excitation wavelength is shorter than 860 nm, the electron/hole pairs are generated in (6, 5) both SWCNT and n-type GaAs, and then will be separated and transported to the external circuit under the action of the built-in electric field at the interface. The photogenerated holes in n-type GaAs drift towards the (6, 5) SWCNT side, and then are collected by electrodes and transported to the external circuit. However, when the excitation wavelength of laser exceeds the absorption limit of n-type GaAs, the optical absorption of the device mainly comes from (6, 5) SWCNT film, the photo-induced electron-hole pairs are separated by the built-in electric field at the SWCNT/GaAs heterojunction interface, and the photo-induced electrons are transferred to the external cir-

cuit through n-type GaAs. The existence of graphene is conducive to reduce the probability of photo-generated carrier combination during the transport in SWCNT film so that more holes will be transport to the external circuit. Therefore, when the excitation wavelength is larger than 860 nm, the graphene/(6, 5) SWCNT film dominates the photoelectric response process.

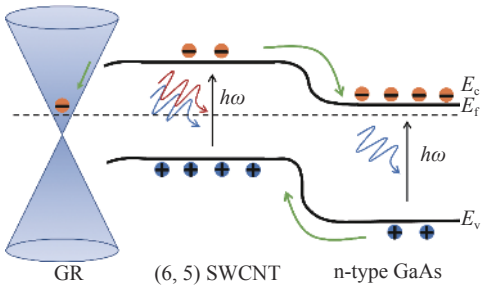

Fig. 6　Schematic diagram of the energy band structure of graphene/SWCNT film/GaAs vdW heterojunction exposed to light irradiaton

图 6　石墨烯/SWCNT 膜/GaAs vdW 异质结在光照时的能带结构示意图

4　Conclusion

In conclusion, we report a self-powered photodetector based on graphene/SWCNT film/GaAs vdW heterojunction, in which, the p-n junction formed by (6,5)-enriched SWCNT film and n-type GaAs plays a dominate role, while graphene is used to reduce the probability of carrier recombination in SWCNT film and promote the carrier transport. The experimental results show that the self-powered photodetector based on graphene/SWCNT film/GaAs vdW heterojunction exhibits a sensitive photoelectric response to 405−1 064 nm visible-near infrared light, breaking through the absorption limit of GaAs, and demonstrating the feasibility of further broadening the spectral response range of a GaAs-based photodetector based on vdW heterojunction. The photoelectric responsivity and specific detectivity of the device under 405 nm laser irradiation can reach 1.214 A/W and 2×10^{12} Jones respectively. It may be attributed mainly to the light absorption of n-type GaAs and the formation of vdW heterojunction. By further optimizing the structure and parameters, the devices based on graphene/SWCNT film/GaAs vdW heterojunctions are expected to be used as high-efficiency solar cells and wide-spectrum photodetectors.

——中文对照版——

1　引　言

作为典型的准一维纳米材料，单壁碳纳米管(SWCNT)根据其直径和手性表现出半导体型和金属型，而且半导体型 SWCNT 为直接带隙且其带隙与直径成反比例关系[1-2]，超高的载流子迁移率(10^5 cm^2 / Vs)、高吸收系数(10^4−10^5/cm)和长激子扩散长度使得 SWCNT 被广泛应用于构筑高性能光电器件[3-5]。但是，较强的库仑相互作用导致 SWCNT 吸收光子后所形成的光生电子/空穴对以激子的形式存在，其数百 meV 的激子结合能受 SWCNT 直径直接影响[6-8]。为了促进激子的有效分离，通常采用施加强电场或构建异质结的方式以便形成较强的内建电场。尤其是，通过与其他材料(例如体半导体、纳米材料和聚合物)构建异质结的策略被广泛用于增强激子分离和载流子输运[9-16]。

在 SWCNT 基异质结中，SWCNT /n 型体半导体范德华(van der Waals, vdW)异质结可以同时利用 SWCNT 的超高载流子迁移率以及体半导体的优异光电性能，具有结构简单、工艺简便、易于调控界面等优点[12-18]。更重要的是，这种新型器件结构突破了传统 pn 结在生长工艺中所受晶格匹配的限制，而且还可以避免 vdW 异质结形成过程中原子相互扩散导致的界面无序结构，进而有利于光生载流子在界面处的分离和输运[19-20]。因此，基于 SWCNT /体半导体 vdW 异质结的光电器件有望表现出更高的光电响应特性[17-18]。另外，通过调控 SWCNT 的直径/手性、费米能级等参数可以与体半导体形成能带匹配、具有原子级界面的新型混合维度 vdW 异质

结，有利于开发更高性能的新型宽光谱光电器件。

与间接带隙半导体硅不同，砷化镓(GaAs)是一种具有更优异光电性能的直接带隙光电半导体，其具有更合适的带隙和更高的载流子迁移率，并已经被广泛用于高效空间太阳能电池。因此，基于 SWCNT/GaAs vdW 异质结的光电器件有望比硅基 vdW 异质结光电器件表现出更高的光电响应特性。Liang 等[21] 首先证明了在单根 SWCNT/n-GaAs 异质结中有很强的整流性能，并且在光照下观察到了明显的光伏效应，这为高性能自供电 SWCNT/GaAs 光电探测器奠定了基础。Li 等[22] 报道了单根 SWCNT/n 型 GaAs 异质结的光伏响应。发现载流子传输在低正向偏压下由电子热电子发射占主导，而通过带间状态的空穴隧穿主要在低反向偏压下贡献电流。Behnam 等[23] 研究了基于 SWCNT 薄膜/GaAs 肖特基接触的金属-半导体-金属(MSM)光电探测器，并发现在 260 K 以上的温度条件下，热电子发射是 SWCNT 膜/ GaAs 异质结中的主要传输机制。该探测器在 633 nm 激光辐照和 10 V 偏压条件下表现出 0.161 A/W 的光电响应度和高开关比。

但是，不同直径或混合导电属性碳纳米管的存在导致 SWCNT 薄膜中的载流子极易发生非辐射复合，从而降低了光生载流子的分离和传输效率。因此，本论文采用以(6, 5)手性为主的 SWCNT 薄膜与 n 型 GaAs 构建 p-n 结，并利用石墨烯降低 SWCNT 薄膜内载流子的复合几率和促进载流子传输，构筑了基于这种新型 vdW 异质结的自驱动光电探测器，详细研究了该器件在零偏压条件对可见-近红外波段的宽光谱响应特性。本文研究验证了基于该 vdW 异质结构筑高效太阳能电池的可行性。

2 实验部分

2.1 SWCNT 薄膜制备

SWCNT 薄膜采用真空抽滤的方法制备[24]，具体步骤如下：首先将 0.5 mg (6, 5)手性为主的 SWCNT 粉体(购自 Sigma-Aldrich)分散到十二烷基硫酸钠(SDS)水溶液(0.01 g/mL)中低温超声处理 2 h，并将混合溶液以 14000 r/min 的速度离心 20 min，去除未充分分散的 SWCNT。然后，取 10 mL 离心后的上清液逐步滴加到放置有纤维素膜(0.22 μm)的真空抽滤装置中进行抽滤成膜，待混合溶液滤过后添加过量的去离子水清洗 SWCNT 膜中多余的 SDS，以降低其对 SWCNT 薄膜导电性的影响。最后，将纤维素膜上(6, 5)手性为主的 SWCNT 薄膜放入 40 °C 真空烘箱中干燥 2 h 备用。

2.2 石墨烯/SWCNT/砷化镓 vdW 异质结光电器件构筑

本论文选用背面已沉积 AuGeNi 共晶合金(4 μm)电极的单面抛光 n 型 GaAs 衬底(10 mm×10 mm, 20 μm)构筑 vdW 异质结光电器件。首先将 GaAs 衬底依次用丙酮、异丙醇和去离子水清洗去除表面油污。然后利用原子层沉积技术在 GaAs 衬底正表面上沉积一层厚度为 80 nm 的 Al_2O_3 绝缘层，并且中间开有 3 mm×3 mm 的窗口。随后，将 GaAs 衬底浸入 $(NH_4)_2S$ 溶液中，放置 30 min，以钝化窗口内的 GaAs 表面，并用去离子水清洗去除多余的 $(NH_4)_2S$ 溶液。最后，将上述制备的 SWCNT 薄膜(7 mm×7 mm)转移到图案化窗口上方，直接与 GaAs 直接接触形成 SWCNT /砷化镓 vdW 异质结，并缓慢滴加丙酮浸泡溶解去除纤维素膜。随后将石墨烯通过湿法转移方式转移到 SWCNT 薄膜上表面。最后，在窗口周围的石墨烯表面涂覆银浆以形成欧姆接触，获得石墨烯/SWCNT/GaAs vdW 异质结光电探测器。

2.3 测试与表征

本文使用扫描电子显微镜 (SEM, Zeiss Ultra Plus, Germany) 表征石墨烯/ SWCNT 膜/砷化镓范德华异质结表面的微观形貌；使用 inVia Renishaw 拉曼光谱仪测试异质结的 Raman 峰偏移，其中激发波长是 514 nm；器件的光电性能则使用安捷伦 4156C 半导体参数分析仪在室温条件下进行测量，在 405~1064 nm 激光和 AM1.5G 标准太阳光模拟器辐照下测得电流电压(*I-V*)曲线和电流时间(*I-T*)曲线。器件的频率响应曲线则采用斩波器(4~400 Hz)和数字示波器 (Tektronix, TDS 3052C) 进行测试。

3 结果与讨论

所构筑的石墨烯/SWCNT 薄膜/GaAs vdW 异质结光电器件的结构示意图如图 1(a)所示。可以清楚看出，在该异质结结构中(6, 5)手性为主的 SWCNT 薄膜直接与 n 型 GaAs 形成 p-n 结，这与

之前的 SWCNT 网络/石墨烯/GaAs 异质结光电器件有显著区别，后者所形成的是肖特基异质结[25]。采用(6, 5)手性为主的 SWCNT 薄膜一方面有利于提高器件对小于 GaAs 带隙的波段光子的吸收，另一方面，后续可通过掺杂来调控 SWCNT 薄膜费米能级从而更有利于制备高性能的宽光谱光电探测器。本文中，石墨烯主要起到促进光生载流子在 SWCNT 薄膜传输的作用。图 1(b)为窗口区域内石墨烯/SWCNT 膜/GaAs vdW 异质结表面的 SEM 图片，可以清楚地看到，GaAs 表面 SWCNT 与石墨烯一起形成均匀的网状薄膜，并且没有观察到明显的表面活性剂 SDS 残余，说明 SWCNT 薄膜抽滤过程中 SDS 去除较为干净，这将有助于提高 vdW 异质结器件的光电性能。

首先测试了石墨烯/SWCNT 膜/GaAs vdW 异质结光电探测器在暗态和 AM1.5G 光照条件下的 *J-V* 曲线，结果如图 2 所示。从暗态 *J-V* 曲线可以清楚地看出，器件具有明显的整流效应，表明该器件中(6, 5)手性为主的 SWCNT 薄膜与 GaAs 形成了较好的 p-n 结，需要说明的是器件在第一象限时的电流密度较低。当采用 AM1.5G 标准太阳光辐照时，*J-V* 曲线发生明显向下移动，器件的短路电流密度 J_{sc} 可达 19 mA/cm^2，显示出优异的光伏特性，由此说明，器件具有构筑高效太阳电池的潜力。基于经典的热电子发射原理来分析器件的整流性能：

$$J = J_{st}\left[\exp\left(\frac{qV}{nk_0T}\right)-1\right] \quad , \qquad (1)$$

$$J_{st} = A^{*}T^{2}\exp\left(-\frac{q\phi_{ns}}{nk_0T}\right) \quad , \qquad (2)$$

其中，J_{st} 是反向饱和电流密度，T 是绝对温度，k_0 是玻尔兹曼常数，A^*是有效理查森常数，ϕ_{ns} 是势垒高度。从暗态的 *J-V* 曲线可以得出饱和电流密度 J_{st} 为 9.93×10^{-7} A/cm^2，并且热电子发射在载流子扩散和生成复合机制中起主导作用。但是需要指出的是，在第一象限时器件的电流密度增加急剧下降，这可能与反向结的存在有关系，最终导致该器件的 *J-V* 曲线不同于已有结果，但开路电压并未受到较大影响，仍有 0.63 V。因此，对于本文所构筑的石墨烯/SWCNT 膜/GaAs vdW 异质结，主要用作自驱动光电器件，并详细评价其探测性能。

为了评估石墨烯/SWCNT 膜/GaAs vdW 异质结器件作为自驱动光电探测器的探测性能，测量了室温条件下不同激光波长辐照下的光电响应曲线，结果如图 3 所示(彩图见期刊电子版)。图 3(a)和图 3(b)展示了不同波长激光辐照条件下的石墨烯/SWCNT 膜/ GaAs vdW 异质结光电探测器的典型 *J-V* 曲线。可以清楚地看出，所有 *J-V* 曲线在不同波长激光辐照下均向下移动，表明该 vdW 异质结器件均可产生明显的光伏效应。尤其是，在光功率密度为 30 mW/cm^2 的 405 nm 激光辐照条件下，器件的最大短路电流密度 Jsc 可达到 22.48 mA/cm^2。值得注意的是，该器件在 1 064 nm 激光辐照下仍然能够产生较为明显的光伏效应，*J-V* 曲线下移，突破了砷化镓 860 nm 的吸收极限，这主要是由异质结中(6, 5)手性为主的 SWCNT 薄膜引起的。由此说明，(6, 5)手性为主的 SWCNT 薄膜吸收光子后产生的光生载流子可以在异质结界面处被分离成电子-空穴对，并被导出到外电路形成光电流，主导了器件的光电响应过程。而石墨烯的引入则有利于增强 SWCNT 薄膜内空穴的传输，提高电荷收集能力。因此，后续通过优化石墨烯和 SWCNT 薄膜厚度和费米能级、SWCNT 带隙及其与 GaAs 之间的界面接触，将有望进一步提高长波波段的光电响应特性。图 3(c)和图 3(d)展示了在不同激光波长辐照条件下石墨烯/SWCNT 膜/GaAs vdW 异质结光电器件的稳定性曲线。可以清楚地看出，光电流密度随着激光打开或关闭迅速增加或降低，器件对 405~1 064 nm波段的激光表现出快速的光电响应和优异的光电响应稳定性。而且器件具有较高的开关比，对 406~860 nm 激光辐照时开关比均大于 1.1×10^3，即便采用 1 064 nm 激光辐照时器件的开关比仍有 2.5。

此外，还测试了器件在 200 Hz 频率和 405 nm 激光辐照条件下的瞬态光响应曲线，如图 4 所示。可以看出，光电探测器在开/关状态切换时表现出较快的响应速度；当频率为 200 Hz时，光电响应曲线仍然是完整的，当进一步增大频率时，光电探测器的光电响应未达到最大值便开始下降。由此说明，石墨烯/SWCNT 膜/GaAs vdW 异质结自驱动光电器件的最大响应频率是 200 Hz。另外，根据这个光电响应曲线，可以提取器件的光电响应时间。通常情况下，器件的响应(t_r)/恢复(t_f)时间分别被定义为光电电流上升/下降到最大光电流 90%/10% 时所需的时间，从图 4 曲线可知，

该器件的(t_r)/(t_f)分别为 60 μs 和 910 μs。数十 μs 级的光电响应时间再次表明 SWCNT/GaAs 异质结界面处的超快载流子分离效率以及整个石墨烯/SWCNT 膜/GaAs vdW 异质结光电器件的超高电荷输运效率。

进一步评估了石墨烯/SWCNT 膜/GaAs vdW 异质结光电器件的光电响应度 (R) 和比探测率 (D), 其在不同激光波长辐照条件下的光电响应度和比探测率数值为:

$$R_\lambda = \frac{I_p - I_d}{P_{in}} \quad , \tag{3}$$

$$D^* = \sqrt{\frac{A}{2qI_d}} R_\lambda \quad , \tag{4}$$

其中, I_p 是光电流, I_d 是暗电流, P_{in} 是入射光功率, A 是有效面积 (9 mm^2)。通过改变激光波长和入射功率密度, 石墨烯/SWCNT 膜/GaAs vdW 异质结光电器件的光电响应度和比探测率曲线分别如图 5(彩图见期刊电子版)所示。从图 5(a)~5(b)中的光电响应度曲线可以看到, 器件的光电响应度随着入射功率密度的增加而降低, 这一变化趋势基本符合光电探测器的一般规律, 其原因在于随着入射光功率密度的降低, 入射光可以被器件吸收并被充分转换成光电流。由图 5(a)可以得到该自驱动光电探测器在 405 nm 激光辐照条件下的光电响应度最大可达 1 214 mW/cm^2, 高于已有研究报道的数值[24]。尽管器件在 980~1 064 nm 波段的光电响应度比 405~860 nm 波段低了 3 个数量级, 但这一结果仍然说明了本文所构筑的石墨烯/SWCNT 膜/GaAs vdW 异质结具有进一步拓宽光谱响应范围的可行性, 后续通过优化 SWCNT 与 GaAs 的相对厚度可使两者的光吸收具有相同的数量级, 将有望在 405~1 064 nm 波段实现较高的光电响应度。图 5(c)~5(d)为器件在不同激光波长和光功率密度条件下的比探测率曲线。可以清楚地看出, 比探测率与光电响应度相似, 也随着入射光功率密度的降低而整体上增加, 并且在 405 nm 激光以 5 mW/cm^2 的功率密度辐照下获得了最大比探测率, 为 2×10^{12} Jones。

为了更好地理解石墨烯/SWCNT 膜/GaAs vdW 异质结光电探测器件的工作机理, 从能带结构和界面电荷转移的角度进行分析。由于本文中所采用的 SWCNT 是以(6, 5)手性为主的纯半导体性 SWCNT, 因此分析 SWCNT/GaAs 异质结的能带结构时采用(6, 5)SWCNT 的能带结构来讨论该器件的工作机理。石墨烯的狄拉克点为 4.6 eV, 而 (6, 5) SWCNT 表现出弱 p 型, 其导带为 3.9 eV, 价带为 5.1 eV。n 型 GaAs 费米能级接近其 4.07 eV 的导带, 因此, 该 vdW 异质结的能带结构示意图如图 6 所示。当 (6, 5) SWCNT 和 n 型 GaAs 接触时, 由于两者的导带和价带差异而形成Ⅱ型异质结。根据能带理论, 接触后会发生从 n 型砷化镓到 (6, 5) SWCNT 静态电子转移, 这可以通过拉曼光谱获得证实[24]。在石墨烯/(6, 5) SWCNT 和 n 型砷化镓之间产生了内建电场, 并使 (6, 5) SWCNT 和 n 型 GaAs 的能带弯曲, 当激发波长小于 860 nm 时, (6, 5) SWCNT 和 n 型 GaAs 中均会生成电子/空穴对, 然后在界面处内建电场的作用下分离传输到外电路, n 型 GaAs 中的光生空穴向 (6, 5) SWCNT 侧漂移, 然后被电极收集并传输到外电路。但是, 当激光的激发波长超过 n 型 GaAs 的吸收极限时, 器件的光吸收主要源自 (6, 5) SWCNT 薄膜, 所产生的光生电子空穴对在 SWCNT/GaAs 异质结界面处由于内建电场的作用而发生分离, 光生电子通过 n 型 GaAs 被传输到外电路。石墨烯的存在有利于降低光生空穴在 SWCNT 薄膜传输过程中的复合几率。使得更多的光生空穴传输到外电路。因此, 当激发波长大于 860 nm 时, 石墨烯/(6, 5) SWCNT 薄膜主导光电响应过程。

4 结 论

本文报道了一种基于石墨烯/SWCNT 膜/GaAs vdW 异质结的自驱动光电探测器件, 其中由(6, 5)手性为主的 SWCNT 薄膜与 n 型 GaAs 所形成的 p-n 结起主导作用, 石墨烯起到降低 SWCNT 薄膜内载流子复合几率和促进载流子传输作用。实验结果表明, 基于石墨烯/SWCNT 膜/GaAs vdW 异质结的自驱动光电探测器对 405~1 064 nm 波段的可见-近红外光具有较为灵敏的光电响应, 突破了 GaAs 的吸收极限, 验证了基于该 vdW 异质结进一步拓宽 GaAs 基光电器件光谱响应范围的可行性。器件在 405 nm 激光辐照下的光电响应度和比探测率分别可达 1.214 A/W 和 2×10^{12} Jones, 这主要归因于 n 型砷化镓的光吸收和 vdW 异质结的形成。通过进一步优化器件结构和参数, 基于石墨烯/SWCNT 膜/GaAs vdW

异质结的器件有望被用于构筑高效太阳电池和宽光谱光电探测器。

References:

[1] CAI B F, YIN H, HUO T T, *et al*.. Semiconducting single-walled carbon nanotube/graphene van der Waals junctions for highly sensitive all-carbon hybrid humidity sensors[J]. *Journal of Materials Chemistry C*, 2020, 8(10): 3386-3394.

[2] LEI T, POCHOROVSKI I, BAO ZH N. Separation of semiconducting carbon nanotubes for flexible and stretchable electronics using polymer removable method[J]. *Accounts of Chemical Research*, 2017, 50(4): 1096-1104.

[3] ZHANG J, LIU S Y, NSHIMIYIMANA J P, *et al*.. Observation of van Hove singularities and temperature dependence of electrical characteristics in suspended carbon nanotube Schottky barrier transistors[J]. *Nano-Micro Letters*, 2018, 10(2): 25.

[4] CAI B F, SU Y J, TAO Z J, *et al*.. Highly sensitive broadband single-walled carbon nanotube photodetectors enhanced by separated graphene nanosheets[J]. *Advanced Optical Materials*, 2018, 6(23): 1800791.

[5] YANG L J, WANG SH, ZENG Q SH, *et al*.. Carbon nanotube photoelectronic and photovoltaic devices and their applications in infrared detection[J]. *Small*, 2013, 9(8): 1225-1236.

[6] HE X W, LÉONARD F, KONO J. Uncooled carbon nanotube photodetectors[J]. *Advanced Optical Materials*, 2015, 3(8): 989-1011.

[7] MA Z, HAN J, YAO SH, *et al*.. Improving the performance and uniformity of carbon-nanotube-network-based photodiodes via yttrium oxide coating and decoating[J]. *ACS Applied Materials & Interfaces*, 2019, 11(12): 11736-11742.

[8] LIU Y, WEI N, ZENG Q SH, *et al*.. Room temperature broadband infrared carbon nanotube photodetector with high detectivity and stability[J]. *Advanced Optical Materials*, 2016, 4(2): 238-245.

[9] TUNE D D, FLAVEL B S. Advances in carbon nanotube-silicon heterojunction solar cells[J]. *Advanced Energy Materials*, 2018, 8(15): 1703241.

[10] ZHOU H X, YANG M, JI CH H, *et al*.. Excellent-performance C_{60}/graphene/SWCNT heterojunction with light-controlled enhancement of photocurrent[J]. *ACS Sustainable Chemistry & Engineering*, 2020, 8(10): 4276-4283.

[11] GONG Y P, ADHIKARI P, LIU Q F, *et al*.. Designing the interface of carbon nanotube/biomaterials for high-performance ultra-broadband photodetection[J]. *ACS Applied Materials & Interfaces*, 2017, 9(12): 11016-11024.

[12] LI G H, SUJA M, CHEN M G, *et al*.. Visible-blind UV photodetector based on single-walled carbon nanotube thin film/ZnO vertical heterostructures[J]. *ACS Applied Materials & Interfaces*, 2017, 9(42): 37094-37104.

[13] SCAGLIOTTI M, SALVATO M, DE CRESCENZI M, *et al*.. Influence of the contact geometry on single-walled carbon nanotube/Si photodetector response[J]. *Applied Nanoscience*, 2018, 8(5): 1053-1058.

[14] CHEN J X, OUYANG W X, YANG W, *et al*.. Recent progress of heterojunction ultraviolet photodetectors: materials, integrations, and applications[J]. *Advanced Functional Materials*, 2020, 30(16): 1909909.

[15] PERIYANAGOUNDER D, WEI T C, LI T Y, *et al*.. Fast-response, highly air-stable, and water-resistant organic photodetectors based on a single-crystal Pt complex[J]. *Advanced Materials*, 2020, 32(2): 1904634.

[16] YANG W, CHEN J X, ZHANG Y, *et al*.. Silicon-compatible photodetectors: trends to monolithically integrate photosensors with chip technology[J]. *Advanced Functional Materials*, 2019, 29(18): 1808182.

[17] SALVATO M, SCAGLIOTTI M, DE CRESCENZI M, *et al*.. Single walled carbon nanotube/Si heterojunctions for high responsivity photodetectors[J]. *Nanotechnology*, 2017, 28(43): 435201.

[18] KIM Y L, JUNG H Y, PARK S, *et al*.. Voltage-switchable photocurrents in single-walled carbon nanotube–silicon junctions for analog and digital optoelectronics[J]. *Nature Photonics*, 2014, 8(3): 239-243.

[19] 任智慧, 钟绵增, 杨珏晗, 等. 基于AsP/MoS_2异质结的偏振光电探测器 [J]. 中国光学, 2021, 14(1): 135-144.
REN ZH H, ZHONG M Z, YANG J H, *et al*.. A polarization-sensitive photodetector based on a AsP/MoS_2 heterojunction[J]. *Chinese Optics*, 2021, 14(1): 135-144. (in Chinese)

[20] 陈洪宇, 王月飞, 闫珺, 等. 基于Se和有机无机钙钛矿异质结的宽光谱光电探测器制备及其光电特性研究[J]. 中国光学, 2019, 12(5): 1057-1063.
CHEN H Y, WANG Y F, YAN J, *et al*.. Fabrication and photoelectric properties of organic-inorganic broad-spectrum photodetectors based on Se microwire/perovskite heterojunction[J]. *Chinese Optics*, 2019, 12(5): 1057-1063. (in Chinese)

[21] LIANG CH W, ROTH S. Electrical and optical transport of GaAs/carbon nanotube heterojunctions[J]. *Nano Letters*,

2008, 8(7): 1809-1812.

[22] LI H, LOKE W K, ZHANG Q, *et al*.. Physical device modeling of carbon nanotube/GaAs photovoltaic cells[J]. *Applied Physics Letters*, 2010, 96(4): 043501.

[23] BEHNAM A, JOHNSON J, CHOI Y, *et al*.. Metal-semiconductor-metal photodetectors based on single-walled carbon nanotube film–GaAs Schottky contacts[J]. *Journal of Applied Physics*, 2008, 103(11): 114315.

[24] HUO T T, YIN H, ZHOU D Y, *et al*.. Self-powered broadband photodetector based on single-walled carbon nanotube/GaAs heterojunctions[J]. *ACS Sustainable Chemistry & Engineering*, 2020, 8(41): 15532-15539.

[25] 陶泽军, 霍婷婷, 尹欢, 等. 基于碳管/石墨烯/GaAs双异质结自驱动的近红外光电探测器[J]. 半导体光电, 2020, 41(2): 164-168,172.
TAO Z J, HUO T T, YIN H, *et al*.. Self-powered near-infrared photodetector based on single-walled carbon nanotube/graphene/GaAs double heterojunctions[J]. *Semiconductor Optoelectronics*, 2020, 41(2): 164-168,172. (in Chinese)

Author Biographics:

Huo Tingting (1996 —), female, from Yuncheng, Shanxi Province, master degree, graduated from Nanchang University with a bachelor degree in 2018, and obtained a master degree from Shanghai Jiaotong University in 2021, mainly engaged in the research of optoelectronic devices, van der Waals heterojunction and other fields. Email: huotingitng@sjtu.edu.cn.

霍婷婷(1996—), 女, 山西运城人, 硕士, 2018 年于南昌大学获得学士学位, 2021 年于上海交通大学获得硕士学位, 主要从事光电子器件、范德华异质结等领域的研究。Email: huotingitng@sjtu.edu.cn

Sun Lijie (1983—), male, born in Xinxiang, Henan Province, Ph.D., researcher, obtained his Ph.D. from University of Science and Technology of China in 2010, and is currently the chief researcher of the State Key Laboratory of Space Power Technology, Shanghai Institute of Space Power, mainly engaged in the research of GaAs solar cells, new optoelectronic devices, etc. E-mail: sunlijielu@163.com

孙利杰(1983—), 男, 河南新乡人, 博士, 研究员, 2010 年于中国科学技术大学获得博士学位, 现为上海空间电源研究所空间电源技术国家重点实验室主任研究师, 主要从事砷化镓太阳电池、新型光电器件等领域的研究。E-mail: sunlijielu@163.com

Su Yanjie (1982—), male, from Shangqiu, Henan Province, Ph.D., associate researcher/doctoral supervisor, obtained his Ph.D. from Shanghai Jiaotong University in 2012, and is currently working in the Department of Micro-Nano Electronics, School of Electronic Information and Electrical Engineering, Shanghai Jiaotong University, mainly engaged in the research of nanomaterials and devices. E-mail: yanjiesu@sjtu.edu.cn

苏言杰(1982—), 男, 河南商丘人, 博士, 副研究员, 博士生导师, 2012 年于上海交通大学获得博士学位, 现任职于上海交通大学电子信息与电气工程学院微纳电子学系, 主要从事纳米材料与器件等领域的研究。E-mail: yanjiesu@sjtu.edu.cn